Review Article

Xingxing Wang*, Jiahao Tian, Shuai Li*, Peng He, Naiwen Fang, and Guodong Wen

Weldability of high nitrogen steels: A review

https://doi.org/10.1515/rams-2022-0325 received April 27, 2023; accepted May 11, 2023

Abstract: High nitrogen steel (HNS) have been widely used in many industrial fields in place of stainless steels. As we know, the welding is the main fabricating method of the HNS structural components. In this article, the recent investigations of joining methods of HNS, such as tungsten inert gas welding, melt inert-gas welding, laser welding, laser-arc hybrid welding, friction stir welding (FSW), and brazing method are summarized. First, the effect of nitrogen content in shielding gas, welding wire, and base metal on the evolution of microstructure, mechanical properties, and corrosion susceptibility of fusion welded joints are discussed systemically. Then the existing problem during FSW and brazing process of HNS are analyzed. Additionally, the key issues and future trends in the joining of HNS are proposed. The main purpose of this review is to provide a technical reference and theoretical basis for research and technological development during the welding of HNS.

Keywords: high nitrogen steel, shielding gas, corrosion susceptibility

Peng He: State Key Laboratory of Advanced Welding and Joining, Harbin Institute of Technology, Harbin 150001, China

Naiwen Fang: Harbin Welding Research Institute Co., Ltd., Harbin 150028, China

Guodong Wen: Xi'an Research Institute Co. Ltd., China Coal Technology & Industry Group, Xi'an 710077, China

1 Introduction

High nitrogen steels (HNS) have been widely used in many industrial fields due to favorable mechanical performance and corrosion resistance [1-6]. The definition of HNS is mainly associated with the content of nitrogen in steels. For the type of ferrite and martensite stainless steels, it can be classified as HNS when the nitrogen content is higher than that of 0.08% [7–9]. For the austenitic stainless steels, it can be called HNS when the nitrogen content in austenitic matrix is more than 0.40% [7-9]. With the development of metallurgical technology and invention of new steels, different kinds of steels can be considered as HNS, like the creep resistant steel with the nitrogen content of more than 0.10% or the tool steel with the nitrogen content that exceeds 2.00%. In a word, although the definition of HNS is important, there is still no clear definition that is accepted internationally [10]. In addition, lots of investigations have pointed out that the steel can be described as HNS when the nitrogen concentration is higher than that of liquid standard solubility due to the application of pressurized smelting equipment, and the liquid standard solubility in this definition refers to the values with the temperature of 1,600°C and nitrogen fractional pressure of 0.1 MPa [7-9].

Welding is the main manufacturing technique to join the HNS [11–15]. Lots of welding methods have been carried out to join the HNS, such as tungsten inert gas welding (TIG) [16–18], melt inert-gas welding (MIG) [19–21], laser welding (LW) [22–25], laser-arc hybrid welding [26,27], and friction stir welding (FSW) [4,28–30]. For the conventional fusion welding, the welding defects of porosity, solidification cracks in welded zone. and liquation cracking in heat affected zone (HAZ) cannot be avoided in the welding of HNS [31–34]. For the solid state welding technology of FSW, there are two main welding problems of high strength steels, namely the softening effect in the HAZ and the wear of welding tools [35,36]. The major problem in the brazing of HNS is the formation of brittle intermetallic compounds and the loss of nitrogen.

At present, the investigations on the transformation mechanism of microstructure and mechanical properties of HNS joint are isolated and the concerned research results are scattered, and even some conclusions are

^{*} Corresponding author: Xingxing Wang, Henan International Joint Laboratory of High-Efficiency Special Green Welding, School of Materials Science and Engineering, North China University of Water Resources and Electric Power, Zhengzhou 450045, China; State Key Laboratory of Advanced Welding and Joining, Harbin Institute of Technology, Harbin 150001, China, e-mail: paperwxx@126.com

^{*} Corresponding author: Shuai Li, Henan International Joint Laboratory of High-Efficiency Special Green Welding, School of Materials Science and Engineering, North China University of Water Resources and Electric Power, Zhengzhou 450045, China, e-mail: lyctlishuai@163.com Jiahao Tian: Henan International Joint Laboratory of High-Efficiency Special Green Welding, North China University of Water Resources and Electric Power, Zhengzhou 450045, China

inconsistent [37–39]. Lots of technical problems need to be solved in the welding of HNS. Consequently, it is necessary to summarize the research status on the HNS joint in recent decades. First, the relevant papers of HNS joint are classified according to the welding method. Then the new findings about the HNS joints are sorted out systematically.

This article attempts to present the useful information on the effect of nitrogen in HNS welded joints in perspective. This article mainly discusses the existence form and escape behavior of nitrogen in welded joints and its influence on mechanical properties and corrosion properties. Then try to clarify the relationship between welding parameters, microstructure, and properties based on the references in the last two decades.

2 Current status in the welding of HNS-related materials

The relevant papers and corresponding citations over the years were analyzed with the title key words of "Weld; Nitrogen," calculated from Web of Science data by the end of February 2023, as illustrated in Figure 1. As far as the author is concerned, the investigations on joining of HNS are still a hot issue, especially in the recent 5 years.

3 Joining methods of HNS

3.1 Fusion welding

Fusion welding is widely applied in the structural components of HNS due to better economy and relatively easy operation [40-43]. Lots of investigations have demonstrated that change of microstructure and mechanical performance in HNS welded joints was mainly dominated by the nitrogen content and the difference in critical nitrogen content of joint was attributed to the variation of welding method. In order to regulate the nitrogen content in HNS welded joints, a series of measures have been carried out, including increasing the nitrogen fraction in the mixed shielding gas [44-46], manufacturing different nitrogen content filler metals [47-50], changing the welding parameters [51-53], or preparing different nitrogen content HNS [54]. The investigations have proven that the deterioration of mechanical properties and corrosion resistance of HNS welded joint is associated with the loss of nitrogen. Therefore, nitrogen was always added into the welded joint in the forms of N2 or nitrides to avoid the loss of nitrogen. Then the sound welded joints were obtained due to the control of nitride precipitation, porosity, and ferrite increasing.

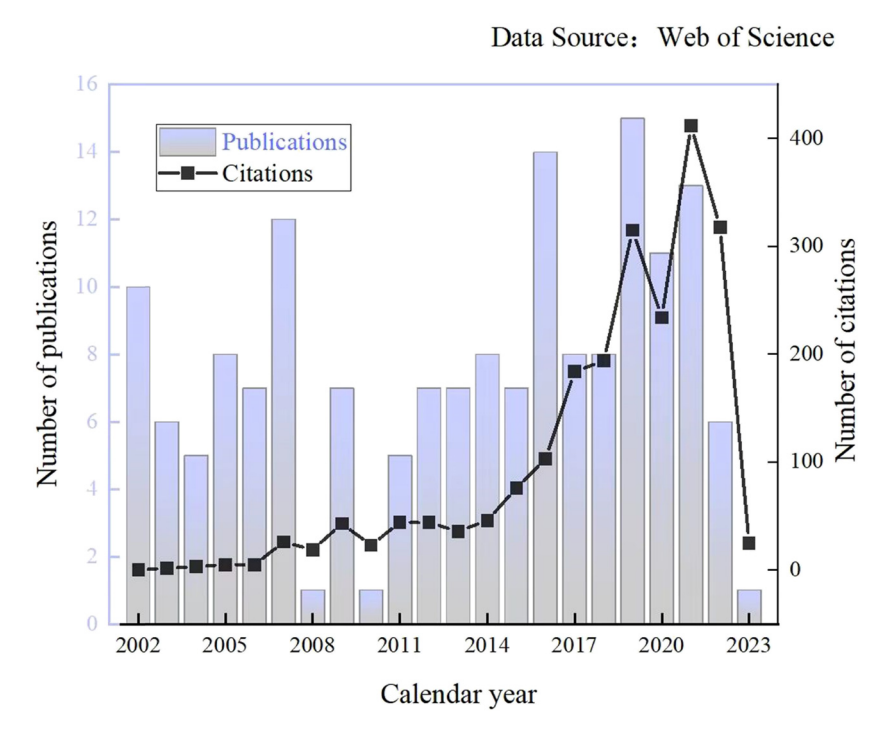


Figure 1: Evolution of relevant papers and citations over the years. Based on Web of Science data by the end of February 2023.

3.1.1 Composition of shielding gas

It is well known that shielding gas has obvious influence on the welded seam forming, welding stability, pore ratio, and mechanical properties [16,23,33,55-57]. Some research showed that the increasing of nitrogen content or the pressure of the nitrogen atmosphere in shielding gas was an effective way to restrain nitrogen loss and porosity in the weld [19]. Reyes-Hernández et al. [3] pointed out that the addition of N2 in protective atmospheres had a slight influence on the impact resistance and fatigue strength of duplex steel 2205 gas tungsten arc welding joint with three different heat inputs. However, the corrosion resistance increased obviously due to the transformation of microstructure, while the ferrite content decreased and the increase of austenite as greater heat input was employed. Zhao et al. [59] found out the nitrogen content increased slightly in the 1Cr22Mn16N CO₂ laser welded joint with the increase of the nitrogen content in shielding gas under the same welding parameters, as shown in Figure 2. However,

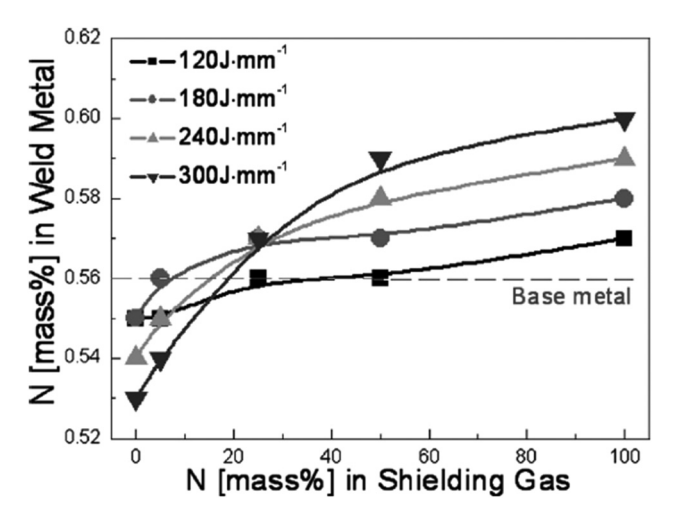


Figure 2: Change of nitrogen content in 1Cr22Mn16N CO₂ laser welded joint with different mixed shielding gas and heat inputs [59].

the nitrogen content in the joint reduced with the increase of the heat input when the shielding gas was pure argon and then opposite change occurred when some nitrogen was added to the shielding gas. In addition, the increase of the nitrogen content in the shielding gas had positive effect in suppressing the appearance of porosity in the welded joint when the nitrogen content is <4.0% [16]. Lai et al. also pointed out that there was no obvious gas pores found in the 2205 duplex stainless steel fiber laser welded joint when the N₂ was added in the shielding gas [45]. Moreover, they also demonstrated that the addition of N2 had no effect on the shape of welded seam, which was nail shape, as shown in Figure 3 [45]. However, in the high nitrogen austenitic stainless steel (HNASS) double-sided synchronous autogenous gas tungsten arc (DSSAG) welded joint, gas pores were detected due to the addition of N2 into shielding gas [60]. Additionally, the welded seam changed obviously in the DSSAG welded joints, which is attributed to the addition of N₂ in the shielding gas, as shown in Figure 4 [60]. The difference of the evolution of welded seam morphology is likely associated with welding method.

Bo et al. [55] studied the effect of shielding gas composition on the stability of laser-arc hybrid HNS welded joints and different shielding gas mixtures were prepared, such as 100% Ar, 95% Ar + 5% N₂, 90% Ar + 10% N₂, 94% Ar + 5% $N_2 + 1\% O_2$, and 89% Ar + 10% $N_2 + 1\% O_2$. The results showed that the nitrogen content in welded seam increased due to the addition of N2. Additionally, they also pointed out that the addition of O₂ had positive effect in the improvement of welding stability and the nitrogen content of welded joint and the best choice of mixed shielding gas was 89% Ar + 10% N_2 + 1% O_2 . In order to avoid the formation of welding porosity, the ultrasonic equipment was used during the fabrication of laser-arc hybrid HNS welded joint and found out that the cavitation and acoustic flow effect promoted the flow of the molten pool and accelerated the nitrogen escaping from the molten pool, while the ultrasonic power should be controlled within a certain range [61].

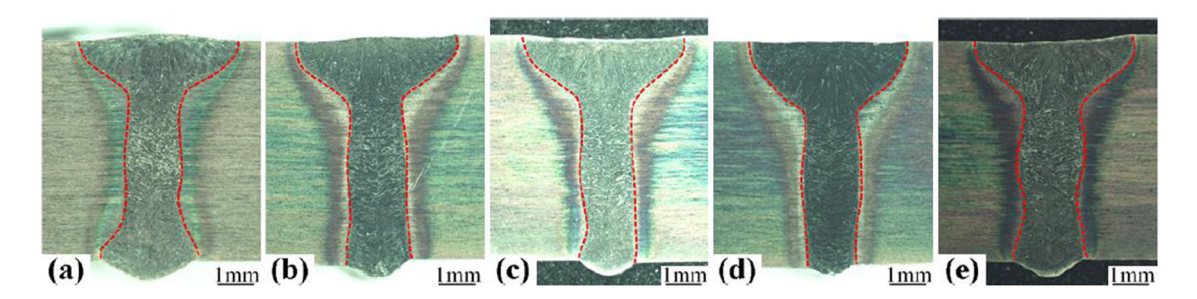


Figure 3: Cross-section of 2205 duplex stainless steel fiber laser welded joint with mixed shielding gas of (a) 100% Ar, (b) 75% Ar + 25% N_2 , (c) 50% Ar + 50% N_2 , (d) 25% Ar + 75% N_2 , and (e) 100% N_2 [45].

4 — Xingxing Wang et al. DE GRUYTER

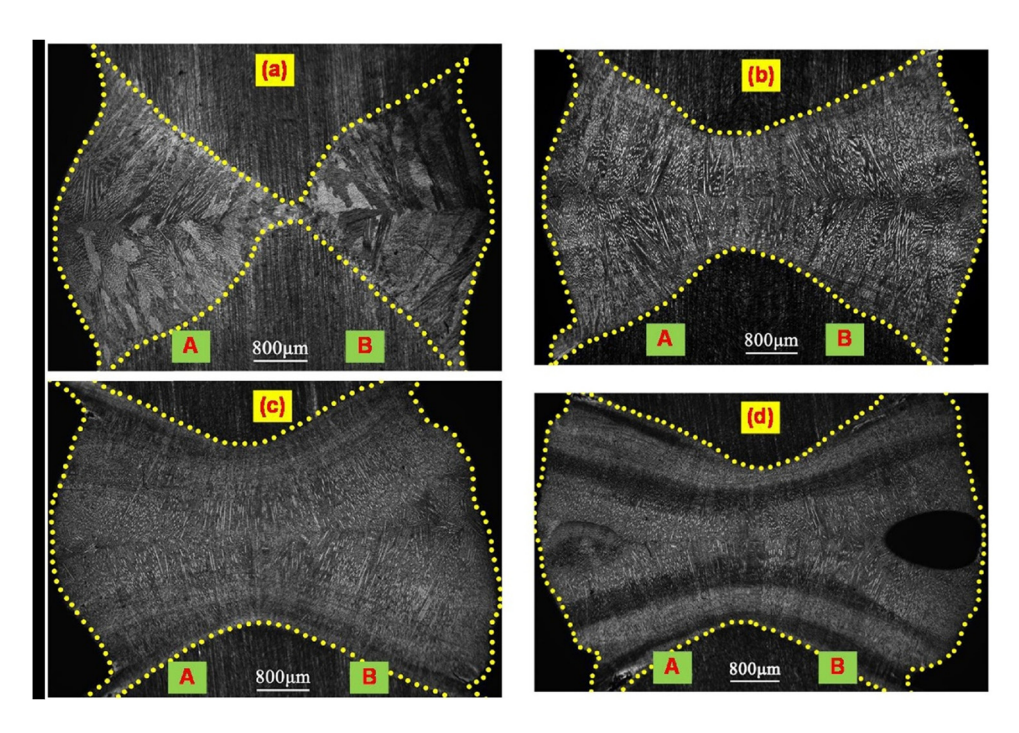


Figure 4: Evolution of cross-sections morphology of joints with mixed shielding gas of (a) 100% Ar, (b) 10% N_2 + 90% Ar, (c) 40% N_2 + 60% Ar, and (d) 100% N_2 [60].

Zou and Zhou [62] also investigated the effect of shielding gas (pure Ar, Ar + 0.4% O₂, and Ar + 0.4% O₂ + 2% N₂) on the weldability of ASTM A240 duplex stainless steel plate TIG welded joint. They demonstrated that the welding efficiencies could be improved obviously owing to the addition of O₂ in the shielding gas and the increase of austenite phase volume fraction is mainly associated with the addition of nitrogen in the shielding gas. Keskitalo et al. [23] have demonstrated that the addition of N₂ to the shielding gas was beneficial to compensate the nitrogen loss during LW process that resulted in the increase of the volume of austenite content of welded joint [23]. They also pointed out that the transformation of microstructure had no obvious influence on the micro-hardness of welded joint but the toughness increased significantly [23]. Additionally, the phenomenon of increase of austenite phase volume fraction was observed in the S32101 duplex stainless steel welded joint using hyperbaric underwater LW system in 0.15 MPa when the pure nitrogen shielding gas was used [63]. Dong et al. also demonstrated that the nitrogen absorption increased with the increase of N₂ in the mixed shielding gas during LW [46,64].

3.1.2 Mechanism of nitrogen adsorption and desorption

The nature of shielding gases during welding has obvious effect in the absorption of nitrogen. The O_2 and CO_2 belong

to oxidizing gases, which can improve the nitrogen absorption of welded seam, while the reducing gas such as hydrogen could suppress the solution of nitrogen into the molten pool [30]. To avoid the loss of nitrogen and the formation of porosity during fusion welding, it is necessary to have a fundamental understanding of the mechanism of nitrogen adsorption and desorption. Many investigations have been conducted to investigate the adsorption and desorption of nitrogen during the welding process. The results showed that this was a complex phenomenon that was influenced by many variables, such as the nitrogen content in the base metal (BM), concentration of active elements on the surface, pressure of nitrogen in the protective atmosphere, nitrogen content in the filler metal, and actual welding process used [3].

Lai *et al.* [45] pointed out that the nitrogen loss during LW with different shielding gas was associated with two processes, namely the evaporation of nitrogen from molten pool to surrounding at the liquid/gas interface and the escaped process by the method of metallic vapor erupting from keyhole, as shown in Figure 5. More specifically, the nitrogen loss was mainly associated with the evaporation process when the shielding gas was pure argon, as shown in Figure 5(a); the nitrogen evaporation reduced obviously when the shielding gas mixed with 50% Ar + 50% N₂ was used and then the movement direction of nitrogen at the liquid/gas interface changed when pure N₂ shielding gas

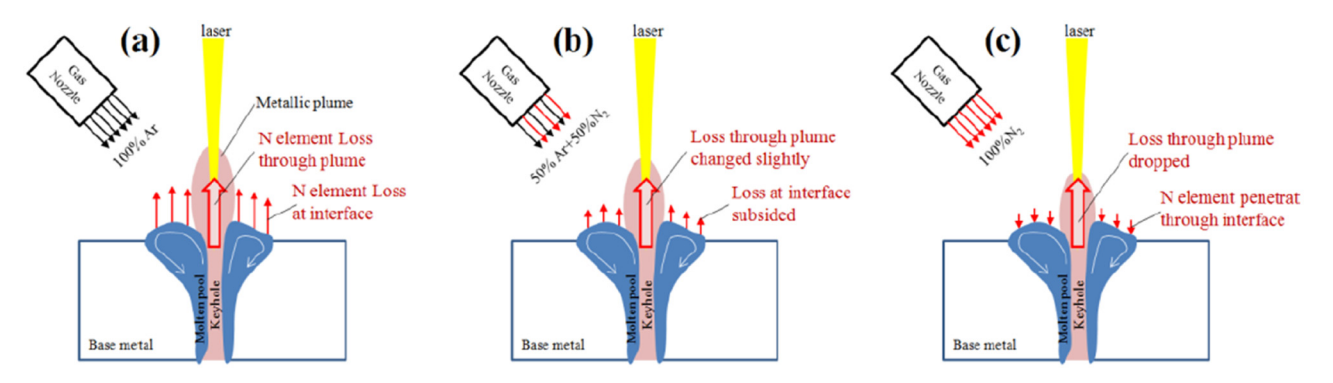


Figure 5: Sketch diagram of nitrogen adsorption and desorption mechanism under different shielding gases: (a) 100% Ar, (b) 50% Ar + 50% N_2 , and (c) 100% N_2 [45].

was applied, as shown in Figure 5(b) and (c), respectively. Similar evolution mechanism of nitrogen was also demonstrated by Qiang and Wang [60], as shown in Figure 6. Both of them pointed out that the change of movement direction of nitrogen was dominated by the N concentration gradient between the mixed shielding gas and liquid metal [45,60].

Then the evolution of austenite content and morphology was different due to the difference of nitrogen absorption and desorption [45,60]. Liu *et al.* [65] also pointed out that the addition of N_2 in the shielding gas could improve the nitrogen content of the weld seam obviously and the volume fraction of austenite content increased, which

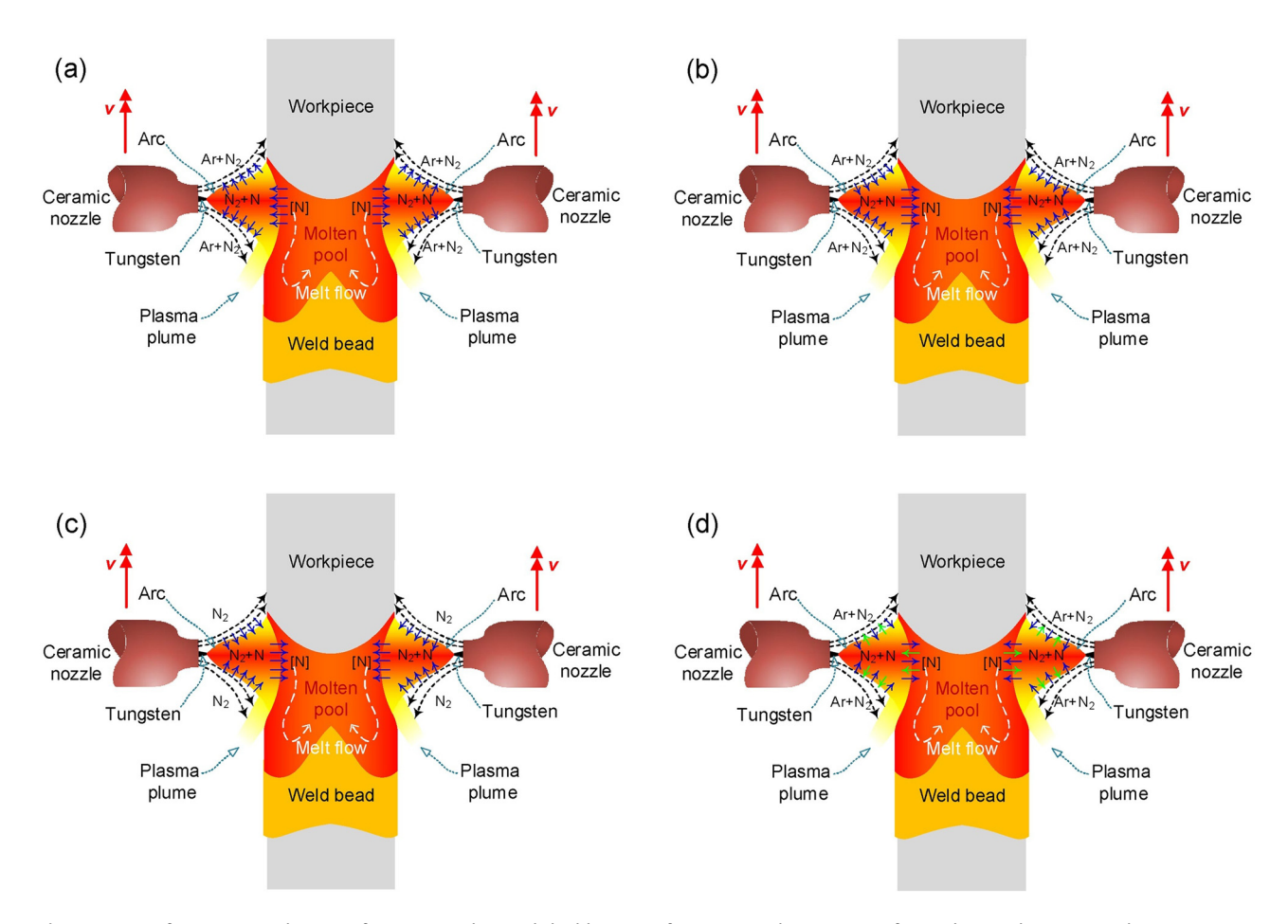


Figure 6: Transformation mechanism of nitrogen with mixed shielding gas of (a) pure Ar, (b) a mixture of Ar and N_2 , and (c) pure N_2 during DSSAGW, and (d) shows ordinary bidirectional movement of N [60].

resulted in the improvement of tensile strength of gas metal arc welded joint of HNS. Moreover, they also concluded that tensile strength was increased by 8.7% when the content of N_2 up to 20%.

It is well known that the solubility of nitrogen in the molten pool is limited. Lai et al. investigated the effect of mixed shielding gas (Ar + N2) on the absorption of nitrogen during 2205 duplex stainless steel LW. They demonstrated that the nitrogen content in the welded seam was less than that in BM even if pure nitrogen was applied [45]. The reason was likely associated with characteristics of LW, such as fast cooling velocity, small molten pool volume, and narrow surface, which had no sufficient time for nitrogen to permeate into the molten pool [45]. However, Zhao et al. pointed out that the nitrogen content in HNS gas tungsten arc welded seam (0.70%) was higher than that of BM (0.56%) [16], which was consistent with the results in ref. [60]. The difference of the absorption ability for nitrogen of the molten pool was associated with the welding method [46,66]. Zhang et al. [67] demonstrated that the nitrogen loss is mainly associated with the Mn evaporation in the cold metal transfer (CMT) welded joint of high nitrogen Cr-Mn steel and the loss of Mn was mainly affected by the peak current than the peak current durations. Specifically speaking, the volatilization of nitrogen will be more than 20% when the loss of Mn was larger than 1%, then resulting in the formation of austenite-ferrite dualphase microstructure.

3.1.3 Nitrogen content of filler materials and BM

In order to solve the nitrogen loss during fusion welding, the nitrogen alloyed filler materials were used. About 7 mm thick nitrogen alloyed austenitic stainless steel 21-4-N butt joint by gas tungsten arc welding (GTAW) with the filler materials of ER2209 (nitrogen alloyed) and E309LMo stainless steel was obtained by Kumar et al. [48]. The mechanical experiments showed that the welded zone exhibited higher hardness and tensile strength with ER2209 filler materials, which attributed to the higher nitrogen content. In ref. [47], three kinds of nitrogenrich filler metals with the nitrogen content of 0.15, 0.60, and 0.90% were designed and then the HNS welded joints were obtained. The mechanical properties experiment results indicated that the highest mechanical properties with the value of 912.5 MPa were acquired when the filler metal with 0.60% nitrogen content was used. Additionally, they also pointed out that nitrogen loss caused by the spatter and fume increased with the increase of nitrogen content in the filler metal.

In order to solve the nitrogen loss causing by the spatters and fume during fusion welding, alloy elements can be added to increase the nitrogen solubility [60,68]. Liu et al. [69] have demonstrated that the addition of MnN into filler metal was useful to promote the transformation of microstructure of HNS GTAW welded joints and the dissolution behavior of MnN is shown in Figure 7. The MnN decomposed during welding and then some of the nitrogen element escaped into the atmosphere with the type of N₂. The residual nitrogen and Mn element entered into the welded seam due to the welding metallurgical reactions [69]. After adding MnN, the formation of ferrite was suppressed and then mechanical properties and impact toughness of welded joint increased by 7.4 and 28.1%, respectively [69]. Li et al. [70] demonstrated that the tensile strength of the HNS laser CMT welded joint increased obviously with the value of 1,198 MPa due to the addition of CrN powder, which was 24.5% higher than that of the non-nitride joint. Additionally, they also pointed out that the volume fraction of ferrite phase reduced with improvement of powder feeding rate and the supplement of N. Moreover, Kamiya et al. [54] pointed out that the loss of nitrogen in high nitrogen austenitic steels during GTAW experiments was associated with the nitrogen contents of base material. The higher nitrogen content always resulted in the higher loss of nitrogen, and the hardness of the weld metal reduced obviously. Additionally, the difference of the loss of nitrogen is attributed to the change of critical pore size of N₂ porosity formation. Liu et al. [71] investigated the effect of three different filler materials of austenitic ER307Mo, duplex ER 2209, and martensitic ER 120S-G on the weldability of HNS and low alloy high strength steel. They demonstrated that the filler material of austenitic ER307Mo was considered to

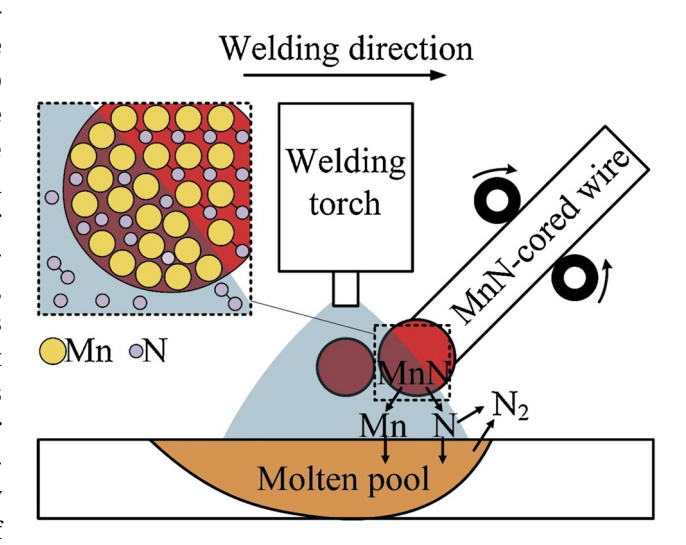


Figure 7: Dissolution behavior of MnN during fusion welding [69].

be the most applicable among the three different candidates, which was mainly attributed to the presence of alloying elements that increase the solubility of nitrogen. Additionally, they also pointed out that the nitrogen diffusion belongs to interstitial diffusion, which had higher diffusion rate.

3.1.4 Welding parameters

It is well known that the properties of welded joint are associated with the welding parameter [72]. Wang et al. [73] investigated the effect of arc and laser energy on the porosity rate of HNS laser-arc hybrid welded seam. The results revealed that the porosity rate increased first and then reduced with the increasing of laser or arc energy. Additionally, the mechanical vibration within a certain frequency range had positive effect which avoids the formation of porosity in HNS laser-arc hybrid welded joints [53]. Hosseini et al. [74] investigated the heat input on the nitrogen loss of duplex stainless steel TIG welded joint. They pointed out that the variation of nitrogen content in the joint was associated with the heat input and the higher heat input resulted in the greater change of nitrogen content in the joint [74] and similar conclusions were obtained by Varbai et al. in the 2205 duplex stainless steel TIG weldment [75,76]. Li et al. [77] investigated the effect of heat input and cooling rate on the microstructure and mechanical properties of HNASS GMAW welded joint using a multistrand composite welding wire. They pointed out that the elongation and tensile strength of welded joints was lower under low heat input and cooling rate than that of the welded joint under high heat input and cooling rate, which attributed to change of volume of ferrite and the precipitation of M₂₃C₆. Kumar et al. [78] also demonstrated that the water quenching after each welding pass had obvious effect on the microstructures of 21-4-N GMAW welded joint, which attributed to the grain coarsening and transformation of carbides.

Jing et al. [19] investigated the effect of nitrogen content in the welded seam on the microstructure and mechanical properties of HNS pulse MIG welded joint by regulating welding parameter. They found out that the welded seam was mainly composed of skeletal-like ferrite and austenite when the nitrogen in the welded seam was lower than 0.24%; then the microstructure transformed to single austenite when the nitrogen was higher than 0.30%. Additionally, they also demonstrated that the pores increased with the increase of nitrogen content and then the impact toughness of welded seam first increased and then decreased. Ming et al. [79] also demonstrated that the

porosity and mechanical properties of HNS MIG welded joint was associated with welding current and nitrogen content of filler metal.

3.1.5 Corrosion behavior

Apart from the mechanical properties, the corrosion resistance of HNS welded joint should be considered in aggressive conditions [35,39,58,80-82]. Reyes-Hernández et al. [3] found out that the addition of N₂ in shielding gas had positive effect to improve the corrosion resistance of duplex steel 2205 gas tungsten arc welded joint in the solution of FeCl₃ + 1% HCl and the ferrite content reduced when higher heat input was applied, which deteriorated the corrosion resistance of welded joint. Bai et al. [83] demonstrated that the corrosion susceptibility of the HNS laser-arc hybrid welded joint decreased in 3.5% NaCl solution when the nitrogen-containing filler metal was used. The investigations have also demonstrated that the corrosion resistance of HNS welded joint was mainly associated with the appearance of depleted-Cr zone, which is caused by the precipitation of M₂₃C₆ along austenite grain boundaries [3,5,45,83–85] and the increase of nitrogen content can promote the formation of austenite, which resulted in the reduction of M23C6 precipitation [85]. Li et al. [85] reported that the precipitation of Cr-rich carbides in the HAZ increased the corrosion susceptibility significantly, which attributed to the low cooling rate and high input. Moon et al. [5,86] investigated the corrosion resistance in the HAZ of Fe-18Cr-10Mn-N austenitic stainless steel through Gleeble simulator systematically. They demonstrated that the interface corrosion susceptibility increased, while the pitting corrosion resistance did not reduce with the increase of δ -ferrite volume, as shown in Figure 8. The reason is that the interface corrosion was dominated not only by the volume of Cr-depletion zone but also the fraction of δ -ferrite and the pitting corrosion was mainly associated with the Cr-depletion zone, which had no obvious change with the increase of δ -ferrite fraction [5,86]. Bai et al. [87] investigated the effect of ultrasonic vibration on the corrosion susceptibility in 3.5% NaCl solution of HNS laser-arc hybrid welded joint, as illustrated in Figure 9. They pointed out that the skeleton-like corrosion morphology in weld seam was associated with the distribution of ferrite dendrites and the HAZ displayed typical grain boundary corrosion features. However, the corrosion susceptibility in weld seam and HAZ decreased obviously after ultrasonic vibration, which attributed to the dendrite refinement and the transformation of solidification model caused by cavitation effect. The AISI 316L(N) austenitic stainless steel GTA welds were obtained with the filler metals of ERNiCrMo-3

8 — Xingxing Wang et al. DE GRUYTER

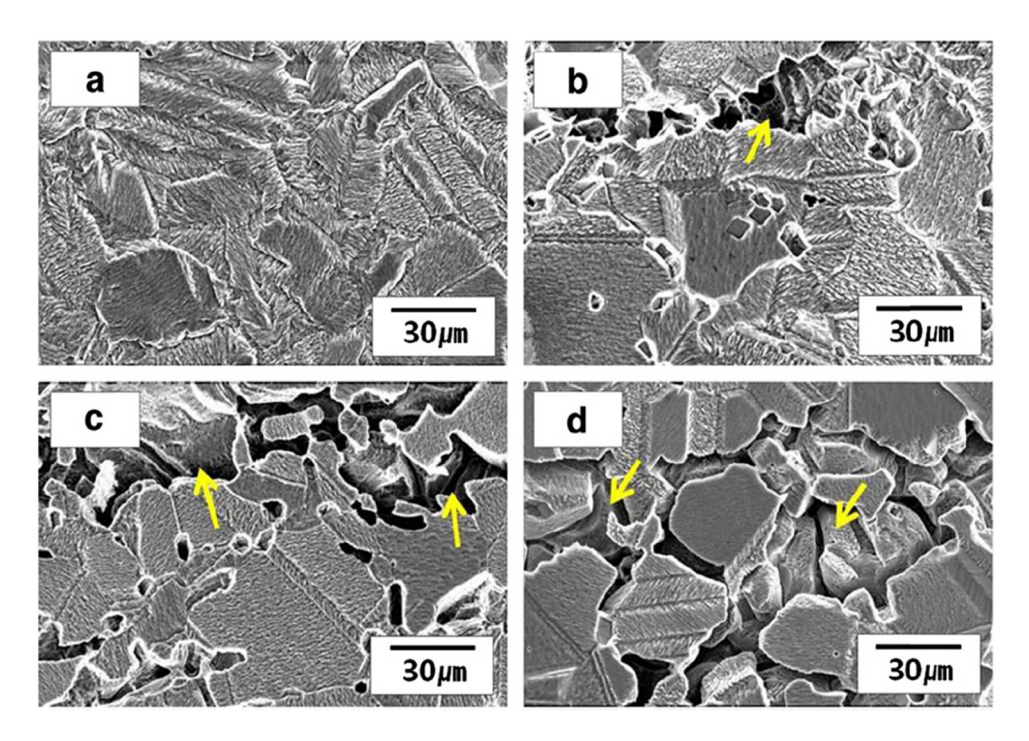


Figure 8: Corrosion behavior of joint after double loop electrochemical potentiokinetic reactivation test in 0.5 M $H_2SO_4 + 0.01$ M KSCN solution: (a) BM and HAZ at different peak temperatures of (b) 1,200°C, (c) 1,300°C, and (d) 1,350°C [86].

and the high temperature corrosion resistance of welded joint were analyzed in 40% K_2SO_4 –60% NaCl for 50 cycles at 650°C [88]. The corrosion resistance of joint with was better than those of BM and joint with ER2594 filler metal.

3.2 **FSW**

According to the above discussion, it is concluded that different kinds of welding defects were formed in the

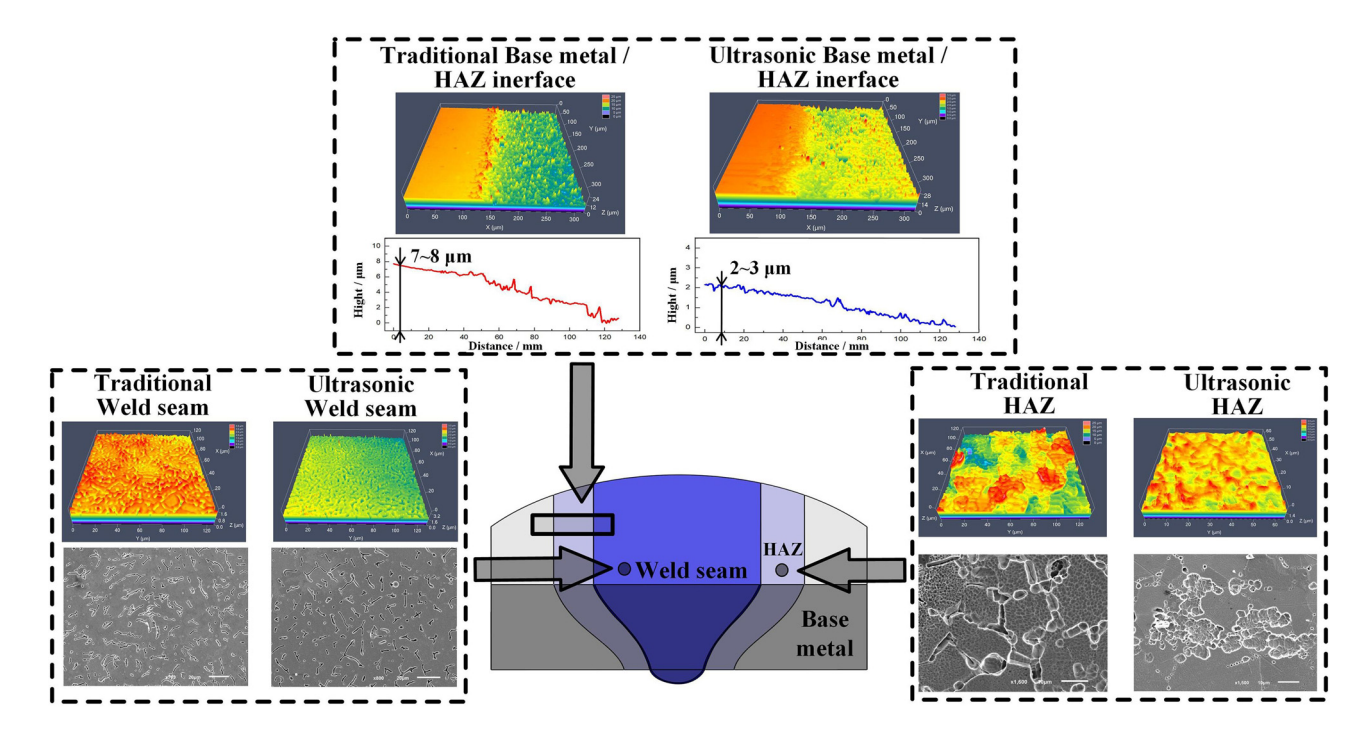


Figure 9: Evolution of corrosion features of HNS laser-arc hybrid welded joint [87].

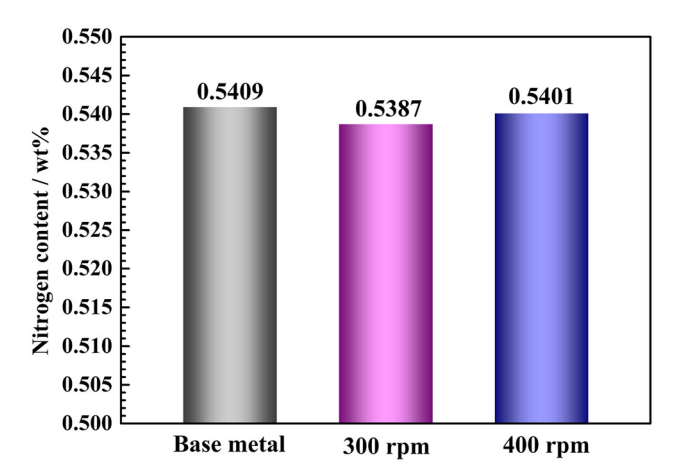


Figure 10: Variation of nitrogen contents in BM and SZ at rotational speeds of 300 and 400 rpm [28].

conventional HNS fusion welded joints, such as nitrogen loss, gas pores, and welding cracking, which always deteriorated the mechanical properties and corrosion resistance of welded joints. The solid state welding technology of FSW suffered to short thermal cycle and exhibited lower peak temperature, which shows positive effect in the suppression of alloy element segregation and the formation of drawbacks. Consequently, the FSW had been widely used to join the HNS [2,28,89,–93].

Li *et al.* [28] investigated the transformation of microstructure and mechanical properties of HNS friction stir welded joints. They demonstrated that sound welded joints were achieved without the appearance of nitrogen loss, as shown in Figure 10, and better comprehensive properties were achieved with the rotational speed of 300 rpm. It was

noteworthy that the strength of friction stir welded joints was higher than that of BM which attributed to the synergistic effect of grain refinement, high density dislocation, and substructure, as shown in Figures 11 and 12, respectively [28]. However, the elongation of both the joints decreased comparing with the BM. Similar results were obtained by Du et al. [94]. They pointed out that the overmatching characteristics were mainly associated with gradient feature of microstructure of FSW joints and post-weld heat treatment was an effective way to reduce the inhomogeneity in the as-welded joints. Then the plastic deformation capacities of the joint increased in coniunction with improved strength [94]. Wang et al. [89] also demonstrated there was no nitrogen loss in the nugget zone of HNS FSW joints and the occurrence of fine dynamically recrystallized grains in the NZ resulted in the improvement of microhardness obviously compared to that of BM.

It is well known that the evolution of welded joints microstructure is mainly dominated by the thermal cycles during welding. In order to investigate the effect of heatinput on the transformation of microstructure and mechanical properties, different heat-input FSW HNS joints were prepared by Zhang et al. [2,95]. In ref. [2], three kinds of heat-input joints were obtained with different welding speeds. They pointed out that the welding speed had obvious effect on the dwell time at elevated temperature, while it had no significant influence on the peak temperature, as shown in Figure 13. In order to regulate the dwell time at high temperature and the peak temperature during FSW, flowing water was applied. The effect of cooling method (aircooled and water-cooled) on the evolution of microstructure and mechanical properties of FSW joints was researched and is as shown in Figure 14. It was evident that the peak

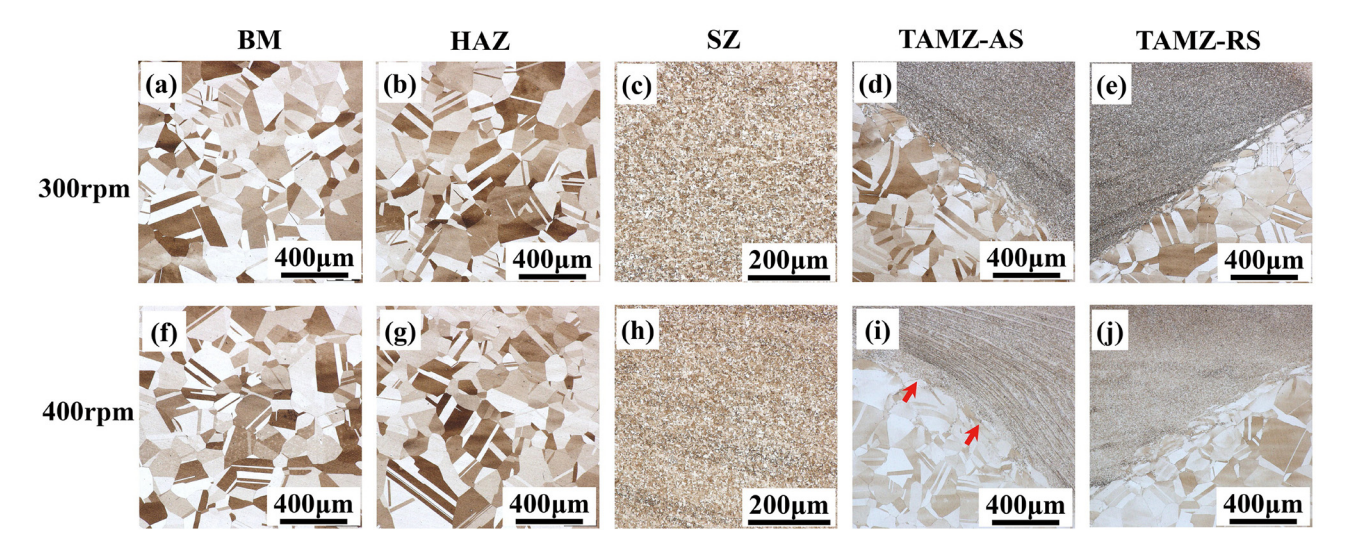
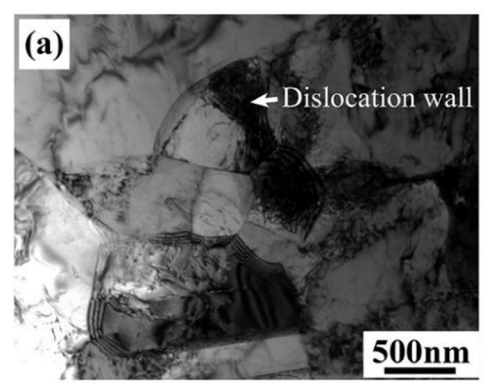


Figure 11: Optical microstructure of different zones of FSW HNS joints: BM (a and f), HAZ (b and g), SZ (c and h), TMAZ-AS (d and i), and TMAZ-RS (e and j) at rotational speeds of 300 and 400 rpm, respectively [28].



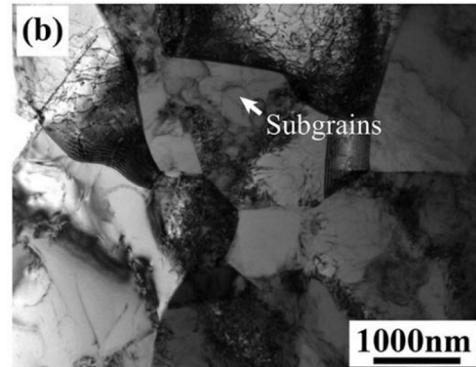


Figure 12: Transmission electron microscope microstructure of FSW specimens at rotational speeds of 300 (a) and 400 rpm (b) [28].

temperature and dwell time at high temperature decreased obviously after the addition of flowing water during welding process compared to air-cooled joint. The microstructural differences were obvious between the air-cooled and water-cooled joints, which is caused by the variation of thermal cycles, as illustrated in Figure 15. They pointed out that the dislocation densities of the HAZs in both FSW joints decreased significantly (Figure 16), which resulted in the reduction of hardness and strength.

As a kind of high-property stainless steel with high strength, plastic deformation capacities, and toughness, the HNS were expected to be used in various industries, especially in aggressive conditions. Therefore, the corrosion susceptibility of FSW joints is also an important factor during the joint safety evaluation apart from strength. Lots of investigations had been carried out to clarify the corrosion mechanism of FSW joints, especially the pitting corrosion.

Zhang *et al.* [96] investigated the pitting corrosion behavior of HNS FSW joints through immersion and electrochemical experiment. They found out that nugget zone displayed better pitting corrosion resistance in 6% FeCl₃

solution than those in the other zones of FSW joints, as shown in Figure 15, which attributed to grain refinement and separation of coarse inclusions during stir process. More specifically, the coarse inclusions were refined and re-dissolved due to the thermal cycle and strong stirring effect during stir process, which is beneficial to inhibit the galvanic corrosion between the inclusions and matrix. Additionally, the grain boundaries were the main diffusion paths of alloy elements and the fine grains in the nugget zone increased the Cr element diffusion rate, and no Cr-depleted zone along ferrite formed. Consequently, the capability of protection and repassivation improved obviously in the fine-grained zone.

Zhang *et al.* [2] also studied the influence of heat-input on corrosion behavior in nugget zone of HNS FSW joints. They found that the evolution of corrosion behavior of nugget zone was mainly associated with the change of heat-input, which is caused by the variation of welding speed. The pitting corrosion mechanism in the immersion solution of 6% FeCl₃ of FSW joint with various heat-input could be demonstrated as in Figure 17. The pitting

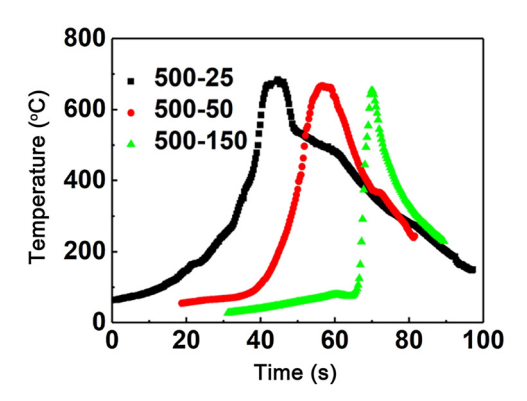


Figure 13: Thermal cycles of HAZs in FSW HNS joints [2].

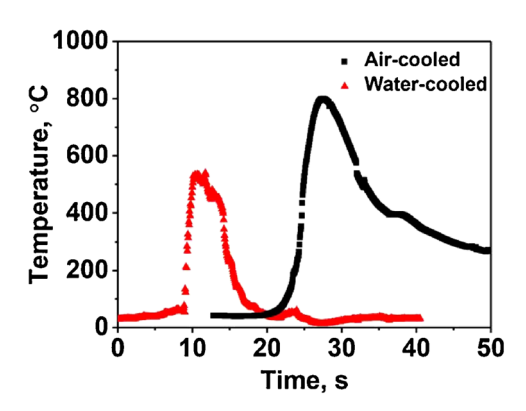


Figure 14: Thermal cycles during FSW of the bottom layer of workpiece near the welding tool pin [95].

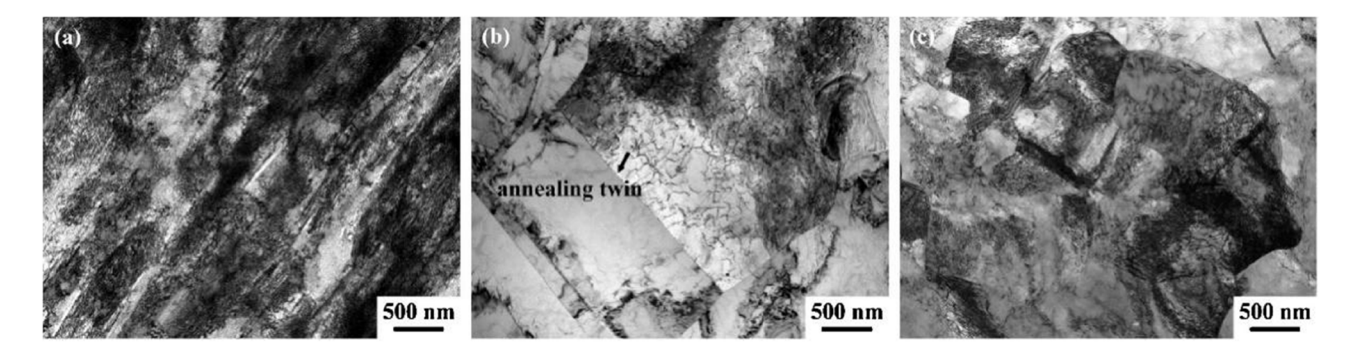


Figure 15: Transmission electron microscope microstructure of (a) HNS, (b) HAZ of air cooling samples, and (c) HAZ of water cooling samples [95].

corrosion of joints were affected by two factors, namely the formation of Cr-depleted zone and distribution of tool wear debris, which is mainly associated with the difference of heat-input caused by welding speed. Generally speaking, the higher the welding speed the lower the heat-input for the FSW joints. For the HNS joints, the corrosion resistance is mainly associated with the formation of Cr-depleted zones near ferrite. The element diffusion improved for the higher heat-input FSW joints, which contributed to the formation of Cr-depleted zones, and the susceptibility to pitting corrosion increased. However, the lower heat-input always led to the severer wear of pin tool and the galvanic corrosion between the increased amount of wear debris and matrix aggravated in the corrosion medium, as displayed in Figure 17. Consequently, the FSW parameters

should be optimized to obtain high-performance joints. Moreover, Zhang *et al.* [95] demonstrated that the cooling method had significant influence on the corrosion behavior of FSW joints, as illustrated in Figure 18. The pitting corrosion of nugget zone in the water-cooled joint was lower than that of air-cooled joint, which attributed to the evolution of tool wear [95]. More specifically, in the water-cooled joint, the hardness of pin tool had no obvious during welding, while the softening effect of pin tool appeared for the air-cooled joint during stir process, which is associated with the difference of high temperature duration and peak temperature, as shown in Figure 14. Furthermore, they found that the corrosion resistance of thermomechanically affected zone (TMAZ) was the weakest area of the FSW joint with the immersion solution of 6%

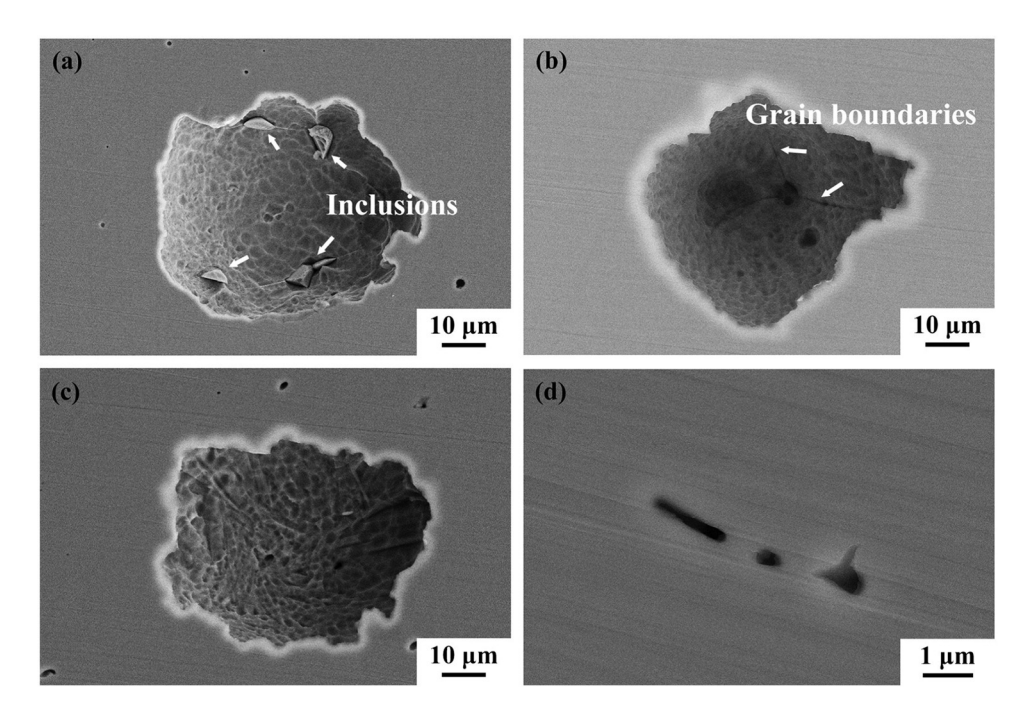


Figure 16: Pitting corrosion morphology of the FSW HNS joint after immersion corrosion experiment in 6% FeCl₃ solution for 72 h: (a and b) BM, (c) HAZ, and (d) NZ [96].

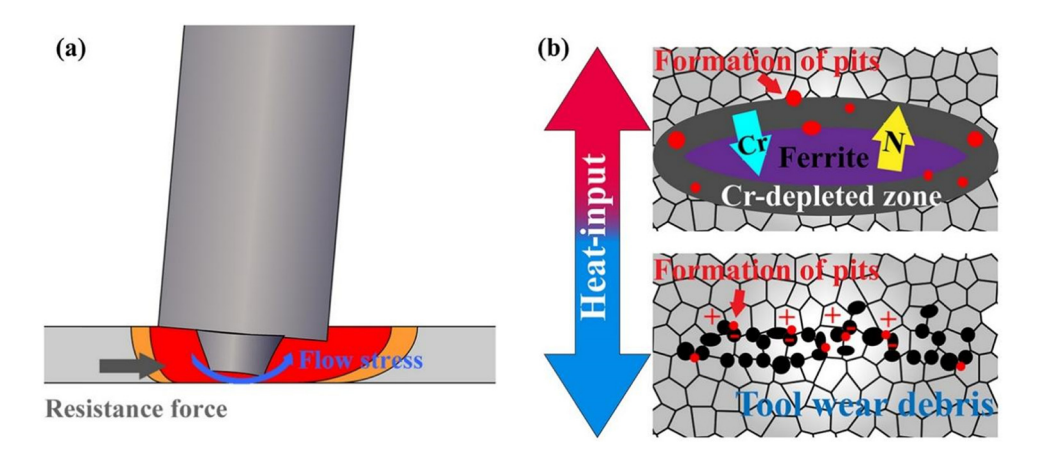


Figure 17: Description of (a) tool wear and (b) formation mechanism of pitting corrosion in FSW HNS welded joints with various heat inputs [2].

FeCl₃, which is attributed to the existence of high defect density and the formation of Cr-rich precipitation, as shown in Figure 19 [97].

3.3 Brazing

Due to the nitrogen loss during fusion welding and the limitation of welding structure shape during FSW, the brazing method was also carried out in the joining of HNS [98–101]. Zhu *et al.* investigated the evolution of microstructure and strength of brazed joints systemically with different kinds of brazing filler metals [98–100]. First, the Ni–Cr–B–Si brazing filler metal was used with the

temperature range of 1,020–1,100°C [98]. They pointed out that the microstructure of brazed joints was mainly composed of BN and Cr_5B_3 compounds and the microstructure evolution mechanism is illustrated in Figure 20. First, the dissolution and diffusion occurred between the filler metal and BMs during wetting process. The BN compounds and Cr-rich solid solution were formed due to the diffusion of alloy elements between the filler metal and substrate (Figure 20a). Then a large number of δ -Fe precipitation were observed, which was caused by the transformation of γ -Fe precipitation (Figure 20b). With the increase of brazing temperature, the solidification of Cr_5B_3 compounds and Ni solid solution occurred in the center of the brazed seam (Figure 20c). Finally, the Fe–Cr compounds were

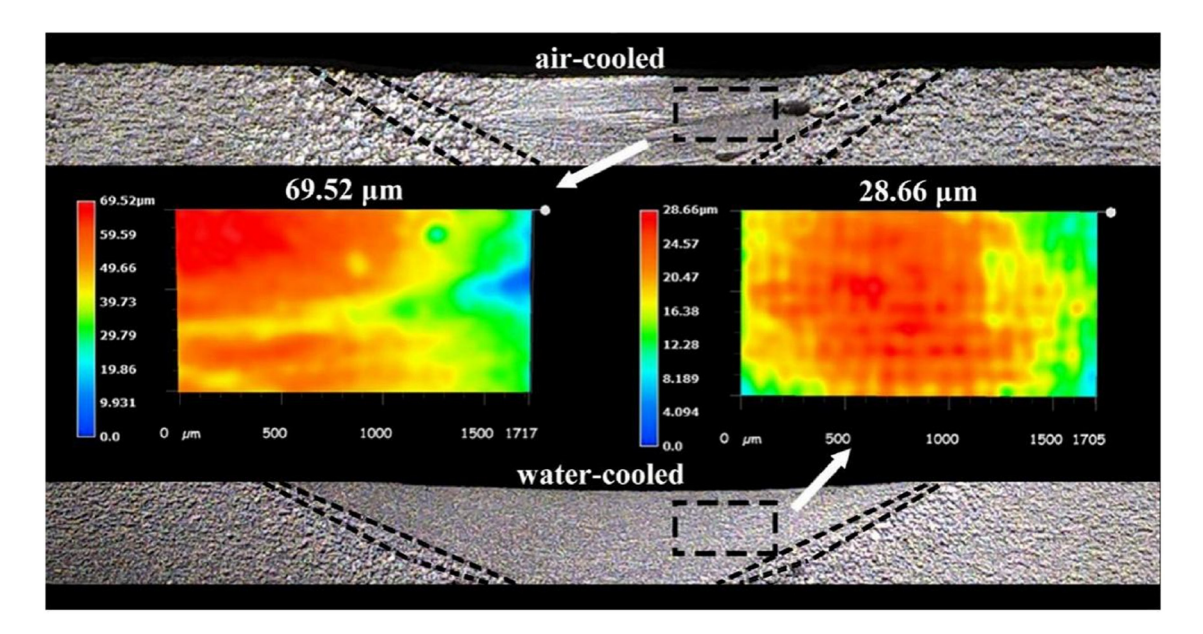


Figure 18: Macroscopic corrosion behavior and the surface characteristics of FSW joints with different quenching conditions after immersion corrosion experiment [95].

DE GRUYTER

Figure 19: (a) Macroscopic corrosion behavior of FSW HNS joint after intergranular corrosion experiment and (b) surface corrosion morphology near the TMAZ [97].

detected in the neighborhood of interface during the cooling process (Figure 20d). Moreover, they also demonstrated that the shear strength of the brazed joints were mainly associated with the evolution of BN compounds and the optimal shear strength of brazed joint was obtained with the value of 176.7 MPa when the brazing temperature was 1,020°C [98].

In order to avoid the negative effect of the formation of BN compounds on the HNS brazed joints, the Ni–Cr–P filler metal was used to obtain a sound HNS brazed joint [99]. They found out that the optimal shear strength of brazed joint was obtained with the value of 163 MPa when the brazing temperature was 1,050°C and the shear strength was mainly dominated

by the evolution of the Cr_2N and (Ni, $Cr)_3P$ compounds [99]. It was noteworthy that the optimal shear strength of HNS were achieved with the value of 290 and 212.4 MPa when the Ag–Cu eutectic filler metal and Ag–Cu–Ni brazing alloy were used [100,101], respectively.

4 Summary and conclusions

In summary, a concise review of the problems in the joining of the HNS was proposed. The results of these

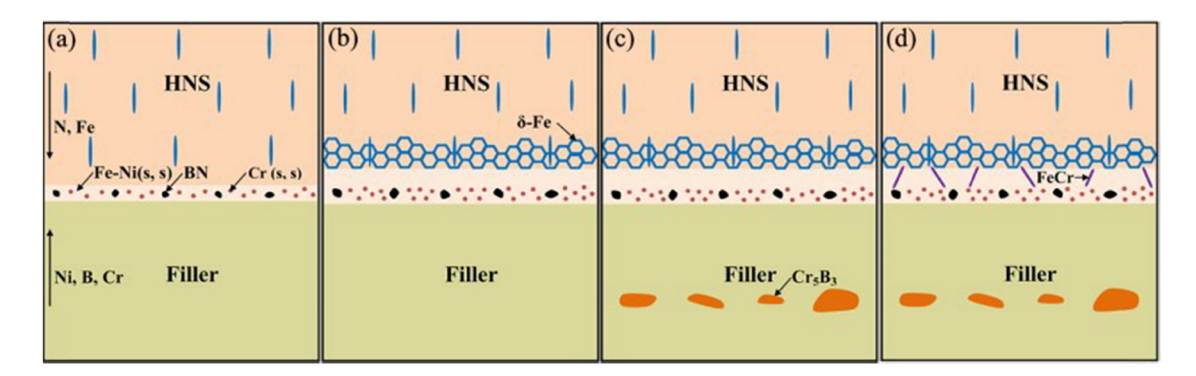


Figure 20: Evolution of intermetallic compounds of HNS and filler metal interface: (a) diffusion stage, (b) reaction stage, (c) solidification stage and (d) cooling stage [98].

investigations have demonstrated that the evolution of microstructure, mechanical performances, and corrosion behavior were mainly dominated by the nitrogen content in the joints. It is feasible to improve the properties of HNS joints by regulating the volume of N₂ in shielding gas, nitrogen content in welding wire, or the welding parameters. The optimal solution of the welding spatter caused by the increase of nitrogen content under the premise of obtaining high performance joints is the key issues in fusion welding. The introduction of external factor in welding process is also an effective way to solve the welding problems of HNS welded joints. The wear of welding tools and the pitting corrosion caused by tool wear debris are the obstacle in the expansion of the application field of FSW. Considering the outstanding performance of brazing method in the joining of HNS sealed container, lots of investigations should be conducted. Furthermore, in order to assess the stability of HNS joints accurately, the fatigue performance and corrosion resistance of joints needs to be further explored. It is well known that the reliability of HNS joints is closely related to the service environment and the revelation of the failure mechanism of joints under service condition is the key theoretical basis for life prediction and evaluation. However, there are few investigations on the reliability assessment of welded joints under service conditions. Consequently, it is necessary to study the evolution of mechanical properties and corrosion resistance HNS joints under service conditions in the future. Additionally, most of the investigations revealed the correlation between microstructure and properties of HNS joints qualitatively, which is of little significance to the actual service conditions. It is important to clarify the correlation between microstructure and properties quantitatively by multi-scale characterization.

Funding information: This research was financially supported by the National Natural Science Foundation of China (52071165, 51705151), Natural Science Foundation Excellent Youth Project and Youth Science Fund Project of Henan Province (Nos. 202300410268 and 202300410272), Project (22HASTIT026) sponsored by the Program for Science & Technology Innovation Talents in Universities of Henan Province, China; Project supported by the Program for the Top Young Talents of Henan Province, China.

Author contributions: All authors have accepted the responsibility for the entire content of this manuscript and approved its submission.

Conflict of interest: The authors state no conflict of interest.

References

- [1] Lang, Y. P., H. P. Qu, H. T. Chen, and Y. Q. Weng. Research progress and development tendency of nitrogen-alloyed austenitic stainless steels. *Journal of Iron and Steel Research International*, Vol. 22, 2015, pp. 91–98.
- [2] Zhang, H., P. Xue, D. Wang, L. H. Wu, D. R. Ni, B. L. Xiao, et al. Effect of heat-input on pitting corrosion behavior of friction stir welded high nitrogen stainless steel. *Journal of Materials Science & Technology*, Vol. 35, 2019, pp. 1278–1283.
- [3] Reyes-Hernández, D., A. Manzano-Ramírez, A. Encinas, V. M. Sánchez-Cabrera, Á. M. de Jesús, R. García-García, et al. Addition of nitrogen to GTAW welding duplex steel 2205 and its effect on fatigue strength and corrosion. *Fuel*, Vol. 198, 2017, pp. 165–169.
- [4] Geng, X., H. Feng, Z. Jiang, H. Li, B. Zhang, S. Zhang, et al. Microstructure, mechanical and corrosion properties of friction stir welding high nitrogen martensitic stainless steel 30Cr15Mo1N. *Metals*, Vol. 6, 2016, id. 301.
- [5] Moon, J., H. Y. Ha, T. H. Lee, and C. Lee. Different aspect of pitting corrosion and interphase corrosion in the weld heat-affected zone of high-nitrogen Fe–18Cr–10Mn–N steel. *Materials Chemistry* and Physics, Vol. 142, 2013, pp. 556–563.
- [6] Sun, G., Y. Zhang, S. Sun, J. Hu, Z. Jiang, C. Ji, et al. Plastic flow behavior and its relationship to tensile mechanical properties of high nitrogen nickel-free austenitic stainless steel. *Materials Science and Engineering: A*, Vol. 662, 2016, pp. 432–442.
- [7] Tang, X. W. Fundamental study on process of Mn18Cr18N retaining ring steel. Doctor's degree, University of Science and Technology Beijing, Beijing, 2017.
- [8] Sun, S. C. Microstructure and mechanical properties of high nitrogen nickel-free austenitic stainless steel. Doctor's degree, Ji Lin University, Ji Lin, 2014.
- [9] Pen, M. D. Study on deformation behavior of high nitrogen austenitic steel. Doctor's degree, Central Iron & Steel Research Institute, Beijing, 2018.
- [10] Park, J. Y., S. J. Park, J. Y. Kang, C. H. Lee, H. Y. Ha, J. Moon, et al. Fatigue behaviors of high nitrogen stainless steels with different deformation modes. *Materials Science and Engineering: A*, Vol. 682, 2017, pp. 622–628.
- [11] Bai, D., F. D. Liu, H. Zhang, and J. Liu. Corrosion behavior and passivation protection mechanism on different zone of highnitrogen steel weld. *Materials Letters*, Vol. 300, 2021, id. 130194.
- [12] Mohammed, R., G. M. Reddy, and K. S. Rao. Welding of nickel free high nitrogen stainless steel: microstructure and mechanical properties. *Defence Technology*, Vol. 13, 2017, pp. 59–71.
- [13] Liu, Y. B., C. Li, X. Y. Hu, C. F. Yin, and T. S. Liu. Explosive welding of copper to high nitrogen austenitic stainless steel. *Metals*, Vol. 9, No. 3, 2019, id. 339.
- [14] Moon, J., T. H. Lee, S. J. Park, J. I. Jang, M. H. Jang, H. Y. Ha, et al. Tensile deformation behavior and phase transformation in the weld coarse-grained heat-affected zone of metastable highnitrogen Fe–18Cr–10Mn–N stainless steel. *Metallurgical and Materials Transactions A: Physical Metallurgy and Materials Science*, Vol. 44, 2013, pp. 3069–3076.
- [15] He, S., D. Yang, Y. Huang, and K. Wang. Effect of the current waveform on the droplet transfer in CMT welding high-nitrogen steel. *Journal of Manufacturing Processes*, Vol. 75, 2022, pp. 41–48.
- [16] Zhao, L., Z. L. Tian, and Y. Peng. Control of nitrogen content and porosity in gas tungsten arc welding of high nitrogen steel.

- Science and Technology of Welding and Joining, Vol. 14, 2009, pp. 87-92.
- [17] Lu, S., W. Dong, D. Li, and Y. Li. Numerical study and comparisons of gas tungsten arc properties between argon and nitrogen. Computational Materials Science, Vol. 45, 2009, pp. 327-335.
- Li, D., S. Lu, D. Li, and Y. Li. Investigation of the microstructure and impact properties of the high nitrogen stainless steel weld. Acta Metalluraica Sinica, Vol. 49, 2013, id. 129.
- [19] Jing, H., K. H. Wang, and W. Qiang. Influence of N-content on microstructure and mechanical properties of PMIG welding joints of high nitrogen steel. Transactions of the China Welding Institution, Vol. 38, 2017, pp. 95-98.
- Zhang, X., Q. Zhou, K. Wang, Y. Peng, J. Ding, J. Kong, et al. Study on microstructure and tensile properties of high nitrogen Cr-Mn steel processed by CMT wire and arc additive manufacturing. Material and Design, Vol. 166, 2019, id. 107611.
- [21] Ning, J., S. J. Na, C. H. Wang, and L. J. Zhang. A comparison of laser-metal inert gas hybrid welding and metal inert gas welding of high-nitrogen austenitic stainless steel. Journal of Materials Research and Technology, Vol. 13, 2021, pp. 1841-1854.
- Sato, Y., W. Dong, H. Kokawa, and T. Kuwana. Nitrogen absorp-[22] tion by iron and stainless steels during YAG laser welding. ISIJ International, Vol. 40, 2000, pp. S20-S24.
- [23] Keskitalo, M., K. Mäntyjärvi, J. Sundqvist, J. Powell, and A. F. H. Kaplan. Laser welding of duplex stainless steel with nitrogen as shielding gas. Journal of Materials Processing Technology, Vol. 216, 2015, pp. 381-384.
- Berezovskaya, V. V., A. V. Berezovskiy, and D. H. Hilfi. Laser [24] welded joints of high-nitrogen austenitic steels: microstructure and properties. Solid State Phenomena, Vol. 284, 2018, pp. 344-350.
- [25] Mohan, D. G., J. Tomków, and S. S. Karganroudi. Laser welding of UNS S33207 hyper-duplex stainless steel to 6061 aluminum alloy using high entropy alloy as a filler material. Applied Sciences, Vol. 12, 2022, id. 2849.
- [26] Wang, J. Y., T. Qi, C. L. Zhong, H. Zhang, X. R. Li, and F. D. Liu. Study on seam nitrogen behavior of high nitrogen steel hybrid welding. Optik, Vol. 242, 2021, id. 167026.
- [27] Sun, S., S. Liu, D. Jia, H. Zhang, and F. Liu. Multiple nonlinear regression model of weld bead shape for high nitrogen steel by laser-arc hybrid welding. Chinese Journal of Mechanical Engineering, Vol. 51, 2015, pp. 67-75.
- [28] Li, H., S. Yang, S. Zhang, B. Zhang, Z. Jiang, H. Feng, et al. Microstructure evolution and mechanical properties of friction stir welding super-austenitic stainless steel S32654. Material and Design, Vol. 118, 2017, pp. 207-217.
- [29] Li, Y., D. X. Du, and R. D. Fu. Effect of post-welded heat treatment on the microstructures and mechanical properties of friction stir welded joint of high-nitrogen austenitic stainless steel. Chinese Journal of Mechanical Engineering, Vol. 51, 2015, pp. 47-53.
- Woo, I. and Y. Kikuchi. Weldability of high nitrogen stainless steel. ISI/ International, Vol. 42, 2002, pp. 1334-1343.
- [31] Cui, B., S. Liu, F. Zhang, T. Luo, and M. Feng. Effect of welding heat input on pores in laser-arc hybrid welding of high nitrogen steel. The International Journal of Advanced Manufacturing Technology, Vol. 119, 2021, pp. 421-434.
- Kumar, N., N. Arora, and S. K. Goel. Weld joint properties of nitrogen-alloyed austenitic stainless steel using multi-pass GMA welding. Archives of Civil and Mechanical Engineering, Vol. 20, 2020, pp. 1-3.

- Zhang, Z., H. Jing, L. Xu, Y. Han, L. Zhao, and C. Zhou. Effects of nitrogen in shielding gas on microstructure evolution and localized corrosion behavior of duplex stainless steel welding joint. Applied Surface Science, Vol. 404, 2017, pp. 110-128.
- [34] Sales, A. M., E. M. Westin, and B. L. Jarvis. Effect of nitrogen in shielding gas of keyhole GTAW on properties of duplex and superduplex welds. Welding in the World, Vol. 61, 2017, pp. 1133-1140.
- [35] Hazra, M., K. S. Rao, and G. M. Reddy. Friction welding of a nickel free high nitrogen steel: influence of forge force on microstructure, mechanical properties and pitting corrosion resistance. Journal of Materials Research and Technology, Vol. 3, 2014, pp. 90-100.
- [36] Yousefian, S., A. Zarei-Hanzaki, A. Barabi, H. R. Abedi, M. Moallemi, and P. Karjalainen. Microstructure, texture and mechanical properties of a nickel-free high nitrogen duplex stainless steel processed through friction stir spot welding. Journal of Materials Research and Technology, Vol. 15, 2021, pp. 6491-6505.
- [37] Li, J., H. Li, W. Peng, T. Xiang, Z. Xu, and J. Yang. Effect of simulated welding thermal cycles on microstructure and mechanical properties of coarse-grain heat-affected zone of high nitrogen austenitic stainless steel. Materials Characterization, Vol. 149, 2019, pp. 206-217.
- [38] Fengde, L., L. Xingran, L. Youzhi, L. Shuangyu, Z. Hong, L. Xinxin, et al. Study of the microstructure and impact properties of the heat-affected zone of high nitrogen steel for laser-arc hybrid welding. Materials Research Express, Vol. 6, 2019, id. 076505.
- [39] Mohammed, R., K. Srinivasa Rao, and G. Madhusudhan Reddy. Studies on fusion welding of high nitrogen stainless steel: microstructure, mechanical and corrosion behaviour. IOP Conference Series: Materials Science and Engineering, Vol. 330, 2018, id. 012035.
- [40] Li, H., W. Xing, X. Yu, W. Zuo, L. Ma, P. Dong, et al. Dramatically enhanced impact toughness in welded ultra-ferritic stainless steel by additional nitrogen gas in Ar-based shielding gas. Journal of Materials Research, Vol. 31, 2016, pp. 3610-3618.
- Moon, J., T. H. Lee, and H. U. Hong. Hot ductility behaviors in the [41] weld heat-affected zone of nitrogen-alloyed Fe-18Cr-10Mn austenitic stainless steels. Metallurgical and Materials Transactions A, Vol. 46, 2015, pp. 1437-1442.
- Muthupandi, V., P. Bala Srinivasan, S. K. Seshadri, and S. [42] Sundaresan. Effect of nitrogen addition on formation of secondary austenite in duplex stainless steel weld metals and resultant properties. Science and Technology of Welding and Joining, Vol. 9, 2013, pp. 47-52.
- Kodama, S., K. Sugiura, S. Nakanishi, Y. Tsujimur, M. Tanaka, and [43] A. B. Murphy. Effect of plasma heat source characteristics on nitrogen absorption in gas tungsten arc weld metal. Welding in the World, Vol. 57, 2013, pp. 925-932.
- Cui, B., T. Luo, and M. Feng. Effect of nitrogen content on the [44] microstructure and properties of the laser-arc hybrid welding joint of high nitrogen steel. Optik, Vol. 243, 2021, id. 167478.
- Lai, R., Y. Cai, Y. Wu, F. Li, and X. Hua. Influence of absorbed [45] nitrogen on microstructure and corrosion resistance of 2205 duplex stainless steel joint processed by fiber laser welding. Journal of Materials Processing Technology, Vol. 231, 2016, pp. 397-405.
- Dong, W., H. Kokawa, Y. S. Sato, and S. Tsukamoto. Nitrogen [46] desorption by high-nitrogen steel weld metal during CO2 laser

- welding. Metallurgical and Materials Transactions B: Process Metallurgy and Materials Processing Science, Vol. 36, 2005, pp. 677–681.
- [47] Liu, Z., C. Fan, C. Chen, Z. Ming, C. Yang, S. Lin, and L. Wang. Design and evaluation of nitrogen-rich welding wires for high nitrogen stainless steel. *Journal of Materials Processing Technology*, Vol. 288, 2021, id. 116885.
- [48] Kumar, N., N. Arora, S. K. Goel, and D. B. Goel. A comparative study of microstructure and mechanical properties of 21-4-N steel weld joints using different filler materials. *Materials Today*, Vol. 5, 2018, pp. 17089–17096.
- [49] Mohammed, R., G. M. Reddy, and K. S. Rao. Effect of filler wire composition on microstructure and pitting corrosion of nickel free high nitrogen stainless steel GTA welds. *Transactions of the Indian Institute of Metals*, Vol. 69, 2016, pp. 1919–1927.
- [50] du Toit, M. Filler metal selection for welding a high nitrogen stainless steel. *Journal of Materials Engineering and Performance*, Vol. 11, 2002, pp. 306–312.
- [51] Zhang, J., W. Xin, G. Luo, R. Wang, Q. Meng, and S. Xian. Effect of welding heat input on microstructural evolution, precipitation behavior and resultant properties of the simulated CGHAZ in high-N V-alloyed steel. *Materials Characterization*, Vol. 162, 2020, id. 110201.
- [52] Vashishtha, H., R. V. Taiwade, S. Sharma, and A. P. Patil. Effect of welding processes on microstructural and mechanical properties of dissimilar weldments between conventional austenitic and high nitrogen austenitic stainless steels. *Journal of Manufacturing Processes*, Vol. 25, 2017, pp. 49–59.
- [53] Li, X., D. Bai, Y. Wang, F. Liu, H. Zhang, and S. Liu. High-nitrogen steel laser-arc hybrid welding in vibration condition. *Materials Science and Technology*, Vol. 36, 2019, pp. 434–442.
- [54] Kamiya, O., Z. W. Chen, and Y. Kikuchi. Microporosity formation in partially melted zone during welding of high nitrogen austenitic stainless steels. *Journal of Materials Science*, Vol. 37, 2002, pp. 2475–2481.
- [55] Bo, C., Z. Hong, and L. Fengde. Effects of shielding gas composition on the welding stability, microstructure and mechanical properties in laser-arc hybrid welding of high nitrogen steel. Materials Research Express, Vol. 5, 2018, id. 096513.
- [56] Kumar Gurrala, A., A. Tirumalla, S. Sheik, and R. Mohammed. Role of nitrogen shielding environment on microstructure and corrosion behavior of 2205 duplex stainless-steel A-GTA welds. *Materials Today: Proceedings*, Vol. 66, 2022, pp. 595–601.
- [57] Wu, S. K., K. Zheng, J. L. Zou, F. Jiang, and X. H. Han. A study of the behavior and effects of nitrogen take-up from protective gas shielding in laser welding of stainless steel. *Journal of Manufacturing Processes*, Vol. 34, 2018, pp. 477–485.
- [58] Kim, S. T., S. H. Jang, I. S. Lee, and Y. S. Park. Effects of solution heat-treatment and nitrogen in shielding gas on the resistance to pitting corrosion of hyper duplex stainless steel welds. *Corrosion Science*, Vol. 53, 2011, pp. 1939–1947.
- [59] Zhao, L., Z. Tian, and Y. Peng. Porosity and nitrogen content of weld metal in laser welding of high nitrogen austenitic stainless steel. *ISIJ International*, Vol. 47, 2007, pp. 1772–1775.
- [60] Qiang, W. and K. Wang. Shielding gas effects on double-sided synchronous autogenous GTA weldability of high nitrogen austenitic stainless steel. *Journal of Materials Processing Technology*, Vol. 250, 2017, pp. 169–181.
- [61] Bo, C. U., Z. H. Hong, L. I. Shuangyu, and L. I. Fengde. Research on control method of nitrogen content and porosity in hybrid welding joint of high nitrogen steel. *Acta Armamentarii*, Vol. 40, 2019, pp. 2311–2318.

- [62] Zou, Y. and X. Zhou. Effects of nitrogen-added double shielding gas and solution treatment on duplex stainless steel weld microstructure of deep-penetration tungsten inert gas welding. Journal of Materials Engineering and Performance, 2022, pp. 1–9.
- [63] Wang, K., X. Jiao, J. Zhu, C. Shao, and C. Li. Effect of nitrogen protection on weld metal microstructure and intergranular behavior of S32101 duplex stainless steel 15 m water depth hyperbaric laser underwater welding. Advances in Mechanical Engineering, Vol. 14, 2022, id. 168781402110729.
- [64] Dong, W., H. Kokawa, Y. S. Sato, and S. Tsukamoto. Nitrogen absorption by iron and stainless steels during CO₂ laser welding. Metallurgical and Materials Transactions B: Process Metallurgy and Materials Processing Science, Vol. 34, 2003, pp. 75–82.
- [65] Liu, Z., C. L. Fan, Z. Ming, C. Chen, A. Liu, C. L. Yang, et al. Gas metal arc welding of high nitrogen stainless steel with Ar–N₂-O₂ ternary shielding gas. *Defence Technology*, Vol. 17, 2021, pp. 923–931.
- [66] Bonnefois, B., L. Coudreuse, and J. Charles. A-TIG welding of high nitrogen alloyed stainless steels: a metallurgically high-performance welding process. Welding International, Vol. 18, 2004, pp. 208–212.
- [67] Zhang, X., H. Dai, X. Wang, Y. Song, M. Duan, Y. Peng, et al. Effect of droplet transition on arc morphology, Mn evaporation and microstructure during the CMT welding with high nitrogen Cr–Mn steel. *Journal of Manufacturing Processes*, Vol. 85, 2023, pp. 527–543.
- [68] Ming, Z., K. H. Wang, W. Wang, C. L. Fan, Y. Q. Wang, and S. Q. Feng. Effect of welding wire compositions on welding process stability and droplet transfer behavior of high nitrogen stainless steel GMAW. *Transactions of the China Welding Institution*, Vol. 39, 2018, pp. 24–28.
- [69] Liu, Z., C. Fan, C. Chen, Z. Ming, A. Liu, C. Yang, et al. Optimization of the microstructure and mechanical properties of the high nitrogen stainless steel weld by adding nitrides to the molten pool. *Journal of Manufacturing Processes*, Vol. 49, 2020, pp. 355–364.
- [70] Li, B., Z. Lei, S. Wu, Y. Chen, Y. Chen, and Y. Xiong. Effect of powder feeding mode on the stability and nitrogen distribution of high nitrogen steel welding process. *Journal of Materials Processing Technology*, Vol. 291, 2021, id. 117002.
- [71] Liu, Z., C. Fan, C. Yang, Z. Ming, Z. Hua, S. Lin, and L. Wang. Investigation of the weldability of dissimilar joint between high nitrogen steel and low alloy steel by comparing filler metals. *Materials Today Communications*, Vol. 35, 2023, id. 105551.
- [72] Zhang, J., W. Xin, G. Luo, R. Wang, and Q. Meng. Significant influence of welding heat input on the microstructural characteristics and mechanical properties of the simulated CGHAZ in high nitrogen V-alloyed steel. *High Temperature Materials and Processes (London)*, Vol. 39, 2020, pp. 33–44.
- [73] Wang, L., F. D. Liu, W. N. Liu, and M. L. Tian. Study on control methods of welding porosity in laser-arc hybrid welding for high nitrogen steels. *Chinese Journal of Mechanical Engineering*, Vol. 52, 2016, pp. 51–60.
- [74] Hosseini, V. A., S. Wessman, K. Hurtig, and L. Karlsson. Nitrogen loss and effects on microstructure in multipass TIG welding of a super duplex stainless steel. *Material and Design*, Vol. 98, 2016, pp. 88–97.
- 75] Varbai, B., T. Pickle, and K. Májlinger. Effect of heat input and role of nitrogen on the phase evolution of 2205 duplex stainless steel weldment. *International Journal of Pressure Vessels and Piping*, Vol. 176, 2019, id. 103952.

- [76] Varbai, B., Y. Adonyi, R. Baumer, T. Pickle, J. Dobranszky, and K. Majlinger. Weldability of duplex stainless steels - thermal cycle and nitrogen effects duplex stainless steel weld microstructures were investigated as a function of weld thermal cycles and shielding gas nitrogen content. Welding Journal, Vol. 98, 2019, pp. 78S-87S.
- Li, J., H. Li, Y. Liang, P. Liu, and L. Yang. The microstructure and mechanical properties of multi-strand, composite welding-wire welded joints of high nitrogen austenitic stainless steel. Materials, Vol. 12, 2019, id. 2944.
- [78] Kumar, N., N. Arora, and S. K. Goel. Study on metallurgical and mechanical aspects of GMA welded nitronic steel under the influence of weld quenching. Journal of Manufacturing Processes, Vol. 56, 2020, pp. 116-130.
- [79] Ming, Z., K. H. Wang, W. Wang, C. L. Fan, and Y. Q. Wang. Effects of nitrogen content and welding current on microstructure and properties of the weld of high nitrogen austenite steel. Transactions of the China Welding Institution, Vol. 40, 2019, pp. 104-108.
- [80] Nage, D. D. and V. S. Raja. Effect of nitrogen addition on the stress corrosion cracking behavior of 904L stainless steel welds in 288°C deaerated water. Corrosion Science, Vol. 48, 2006, pp. 2317-2331.
- [81] Anita, T., H. Shaikh, H. S. Khatak, and G. Amarendra. Effect of heat input on the stress corrosion cracking behavior of weld metal of nitrogen-added AISI type 316 stainless steel. Corrosion, Vol. 60, 2004, pp. 873-880.
- Jegdić, B. V., B. M. Bobić, B. M. Radojković, and B. Alić. Influence of [82] the welding current intensity and nitrogen content on the corrosion resistance of austenitic stainless steels. Materials and Corrosion, Vol. 69, 2018, pp. 1758-1769.
- [83] Bai, D., Z. Yang, M. Chen, H. Zhang, F. Liu, G. Huang, et al. Study on corrosion mechanism of high-nitrogen steel laser-arc hybrid welded joints. Materials Research Express, Vol. 7, 2020, id. 106531.
- Vashishtha, H., R. V. Taiwade, and S. Sharma. Effect of electrodes and post weld solution annealing treatment on microstructures, mechanical properties and corrosion resistance of dissimilar high nitrogen austenitic and conventional austenitic stainless steel weldments. Materials Transactions, Vol. 58, 2017, pp. 182–185.
- Li, J., H. Li, Y. Liang, P. Liu, L. Yang, and Y. Wang. Effects of heat input and cooling rate during welding on intergranular corrosion behavior of high nitrogen austenitic stainless steel welded joints. Corrosion Science, Vol. 166, 2020, id. 108445.
- Moon, J., H. Y. Ha, and T. H. Lee. Corrosion behavior in high heat [86] input welded heat-affected zone of Ni-free high-nitrogen Fe-18Cr-10Mn-N austenitic stainless steel. Materials Characterization, Vol. 82, 2013, pp. 113-119.
- [87] Bai, D., F. Liu, H. Zhang, and J. Liu. Study on corrosion behavior of high nitrogen steel welded joint assisted by ultrasonic vibration. Materials Letters, Vol. 317, 2022, id. 132101.
- [88] Devendranath Ramkumar, K., N. Mehta, S. Shukla, P. Parameswar, V. Jaya Surya, R. Rishi Bharadwaj, et al. Microstructure evolution, structural integrity, and hot corrosion performance of nitrogen-enhanced stainless steel welds. Journal

- of Materials Engineering and Performance, Vol. 28, 2019, pp. 5806-5819.
- [89] Wang, D., D. R. Ni, B. L. Xiao, Z. Y. Ma, W. Wang, and K. Yang. Microstructural evolution and mechanical properties of friction stir welded joint of Fe-Cr-Mn-Mo-N austenite stainless steel. Material and Design, Vol. 64, 2014, pp. 355-359.
- Li, H. B., Z. H. Jiang, H. Feng, S. C. Zhang, L. Li, P. D. Han, et al. Microstructure, mechanical and corrosion properties of friction stir welded high nitrogen nickel-free austenitic stainless steel. Material and Design, Vol. 84, 2015, pp. 291-299.
- [91] Du, D., R. Fu, Y. Li, L. Jing, J. Wang, Y. Ren, et al. Modification of the Hall-Petch equation for friction-stir-processing microstructures of high-nitrogen steel. Materials Science and Engineering: A, Vol. 640, 2015, pp. 190-194.
- [92] Miyano, Y., H. Fujii, Y. Sun, Y. Katada, S. Kuroda, and O. Kamiya. Mechanical properties of friction stir butt welds of high nitrogencontaining austenitic stainless steel. Materials Science and Engineering: A, Vol. 528, 2011, pp. 2917-2921.
- Mohan, D. G. and C. S. Wu. A review on friction stir welding of steels. Chinese Journal of Mechanical Engineering, Vol. 34, 2021,
- [94] Du, D., R. Fu, Y. Li, L. Jing, Y. Ren, and K. Yang. Gradient characteristics and strength matching in friction stir welded joints of Fe-18Cr-16Mn-2Mo-0.85N austenitic stainless steel. Materials Science and Engineering: A, Vol. 616, 2014, pp. 246-251.
- Zhang, H., D. Wang, P. Xue, L. H. Wu, D. R. Ni, B. L. Xiao, et al. [95] Achieving ultra-high strength friction stir welded joints of high nitrogen stainless steel by forced water cooling. Journal of Materials Science and Technology, Vol. 34, 2018, pp. 2183-2188.
- [96] Zhang, H., D. Wang, P. Xue, L. H. Wu, D. R. Ni, and Z. Y. Ma. Microstructural evolution and pitting corrosion behavior of friction stir welded joint of high nitrogen stainless steel. Material and Design, Vol. 110, 2016, pp. 802-810.
- [97] Zhang, H., D. Wang, P. Xue, L. H. Wu, D. R. Ni, B. L. Xiao, et al. Microstructure and corrosion resistance of friction stir welded high nitrogen stainless steel joint. Corrosion, Vol. 75, 2019, pp. 790-798.
- Zhu, W., H. Jiang, H. Zhang, S. Sun, and Y. Liu. Microstructure and [98] strength of high nitrogen steel joints brazed with Ni-Cr-B-Si filler. Materials Science and Technology, Vol. 34, 2017, pp. 926-933.
- Zhang, H., W. Zhu, T. Zhang, C. Guo, and X. Ran. Effect of brazing [99] temperature on microstructure and mechanical property of high nitrogen austenitic stainless steel joints brazed with Ni-Cr-P filler. ISIJ International, Vol. 59, 2019, pp. 300-304.
- Zhu, W., H. Zhang, C. Guo, Y. Liu, and X. Ran. Wetting and brazing characteristic of high nitrogen austenitic stainless steel and 316L austenitic stainless steel by Ag-Cu filler. Vacuum, Vol. 166, 2019, pp. 97-106.
- [101] Wang, X., Z. F. Li, D. Gao, S. Li, J. Peng, X. Yang, et al. Microstructure and joint properties of high-nitrogen steel brazed by AgCuNi filler metal. International Journal of Modern Physics B, Vol. 36, 2022, id. 2250045.